



第14回 若手によるプラズマ研究会
那珂核融合研究所，2011年3月8日

EROコードによるLHDダイバータ モデリングと不純物輸送シミュレーション

G. Kawamura, Y. Tomita, M. Kobayashi, D. Kato
M. Tokitani, S. Masuzaki, A. Kirschner[†] and D. Tskhakaya[‡]

National Institute for Fusion Science, Japan

[†]Institut für Energieforschung-Plasmaphysik, Forschungszentrum Jülich GmbH, Germany

[‡]Institute of Theoretical Physics, University of Innsbruck, Austria

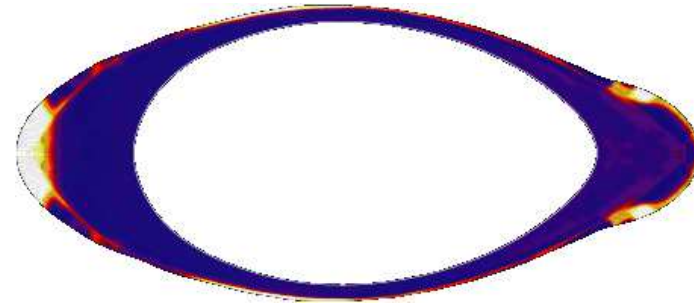
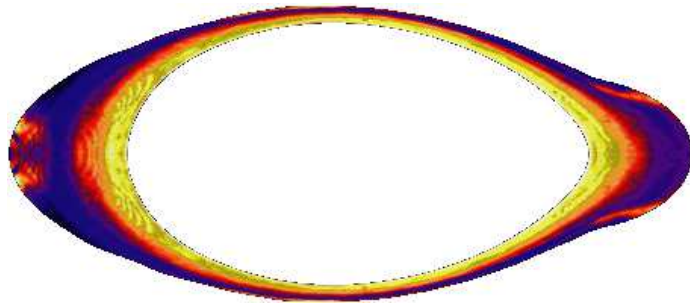
Outline

1. Introduction
2. Modeling of impurity transport simulation in LHD
 - (a) Configuration of LHD divertor
 - (b) Plasma modeling of LHD divertor
3. Impurity transport simulation in LHD diverter
 - (a) Gas puffing simulation
4. Summary and future issues

1.Introduction

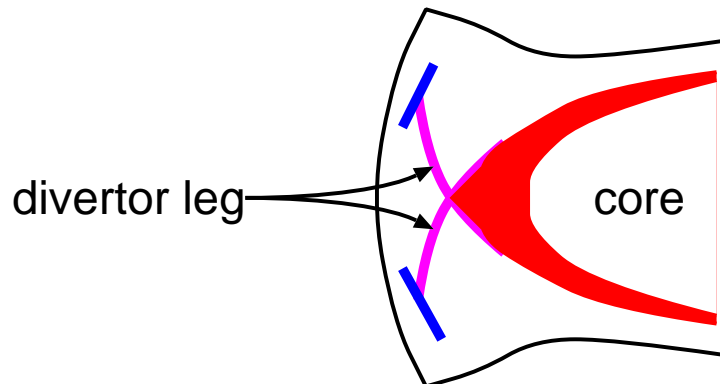
Impurity transport in the LHD edge plasma

§ Carbon density in the ergodic layer (EMC3)



low density case: $n_{\text{LCFS}} = 2 \times 10^{19}\text{m}^{-3}$ high density case: $n_{\text{LCFS}} = 4 \times 10^{19}\text{m}^{-3}$
[M. Kobayashi]

- † Impurity screening due to the parallel flow is found on high density discharges.
- † It could reduce the accumulation of impurity in the core.
- † However, ionization and transport effects of divertor plasmas are not involved yet.



LHD boundary plasma

§ Three characteristic regions in boundary plasma

† Ergodic layer ⇒ EMC3

M. Kobayashi et al., J. Nucl. Mater., 363–365, 294 (2007)

‡ Stochastic magnetic fields

‡ Cross-field diffusion and parallel transport

↕ Interactions

† Divertor leg ⇒ Fluid code (EMC3 in future)

G. Kawamura et al., J. Plasma Fus. Res., 5 (2010) S1020

‡ Parallel flow dynamics

‡ Interactions with neutrals

‡ Recycling

↕ Interactions

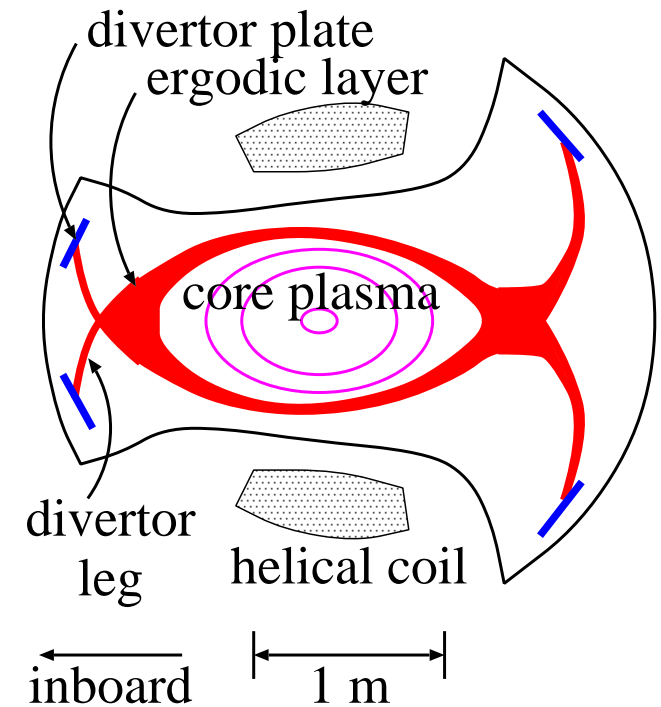
† Impurity around divertor plates ⇒ ERO

G. Kawamura et al., Contrib. Plasma Phys., 50 (2010) 451

‡ Impurity transport

‡ Sputtering

‡ Redeposition

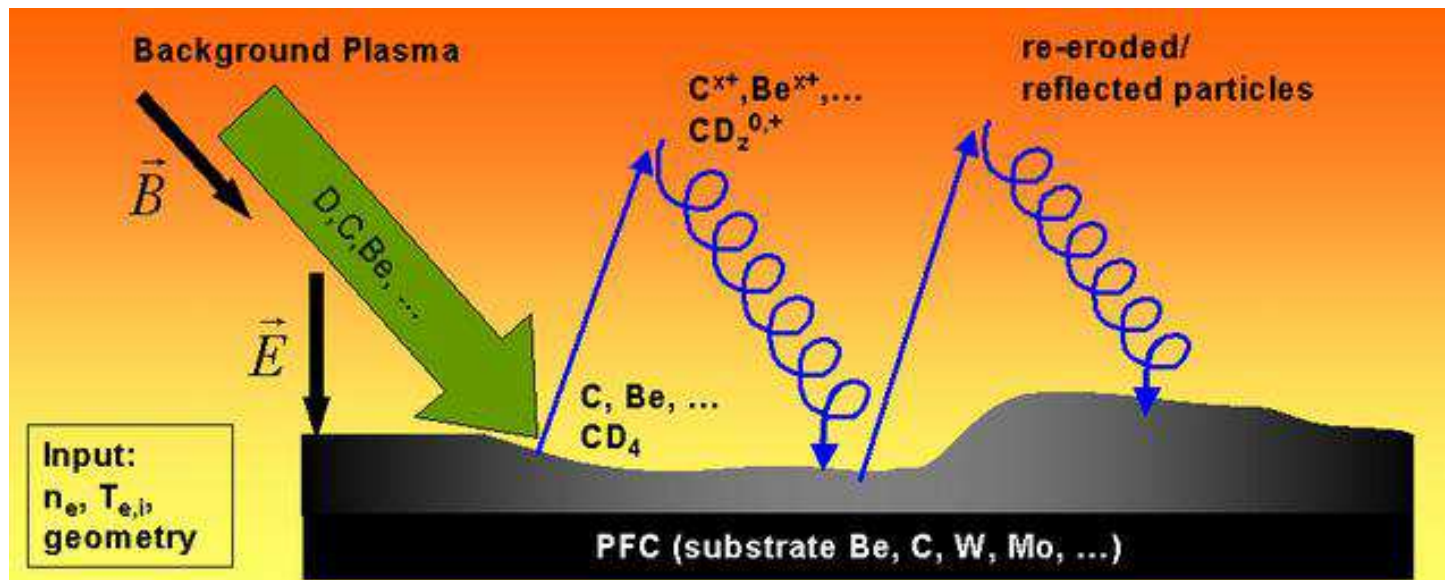


Poloidal cross section of LHD

2. Impurity transport simulation in LHD diverter ERO code (erosion and redeposition)

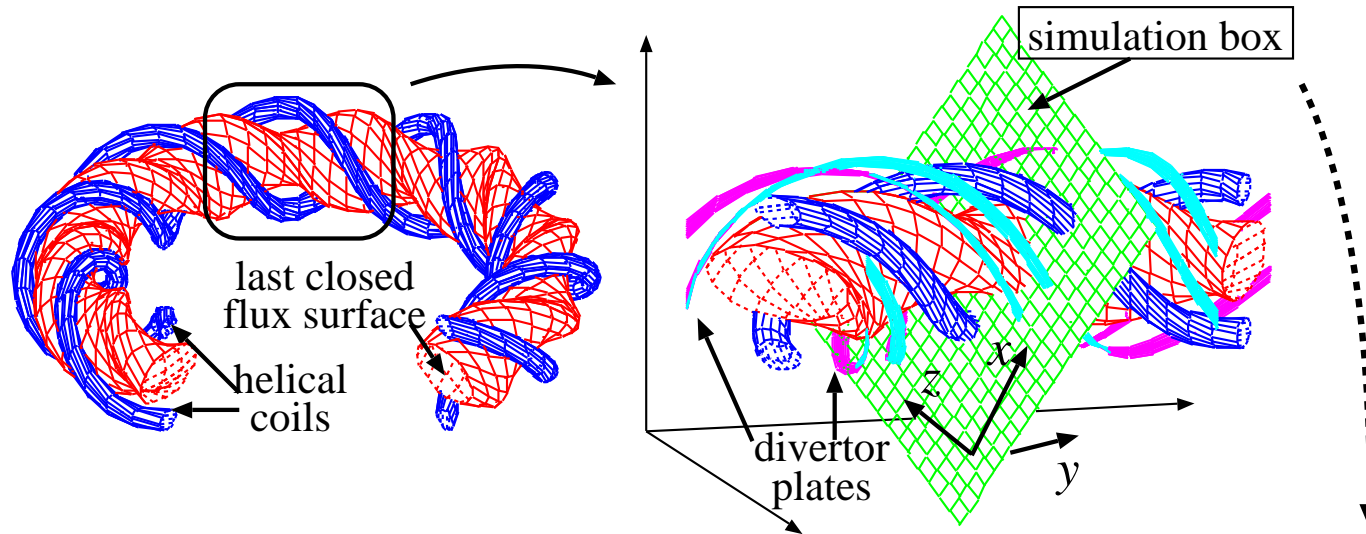
§ Monte Carlo simulation of impurity redeposition on the LHD first wall

- † We employed the ERO code to investigate impurity dynamics in LHD divertor.
A. Kirschner et al., Nuclear Fusion, 40, 989 (2000)
- † Spatial distribution and deposition profile of impurities are available.
- † Impurity particles are sputtered from the plasma facing wall and traced in the simulation by using Newton's equation of motion with various forces; electromagnetic force, friction and thermal forces given by a fixed background plasma.
- † Atomic processes such as ionization and dissociative recombination yield various carbon species; C, C⁺, C²⁺, ..., CH, CH₂⁺, ...



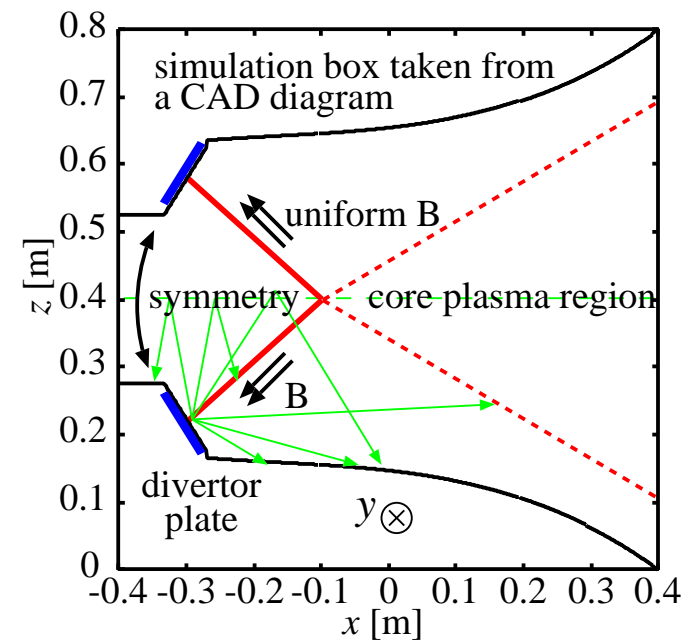
Configuration of the LHD divertor

§ 3D illustrations of the LHD core plasma



§ 2D simulation box

- † The simulation box is chosen to be normal to the divertor plate.
- † With the aid of the up-down symmetry, the lower half of the plane is employed as the simulation box.
- † The impurity particles are reflected at the upper boundary, $z = 0.4$.



Physical models

§ Major components of ERO

† Transport of impurity particles in the plasma

‡ Newton's equation of motion

‡ collisional effects with the background plasma

‡ database of ionization and recombination rates (ADAS)

⇒ These core components are available for any devices.

† Sputtering model

‡ Bohdansky-Yamamura model and SDTimSP code for physical sputtering

‡ Roth model or externally given constant yield for chemical sputtering

⇒ Device-independent, but many uncertainties such as incident-angle effect.

† Background plasma and surface geometry

‡ magnetic field

‡ plasma profiles of n , T_e , T_i , v and gradients of n , T_e and T_i

Parallel electric field is calculated from these gradients.

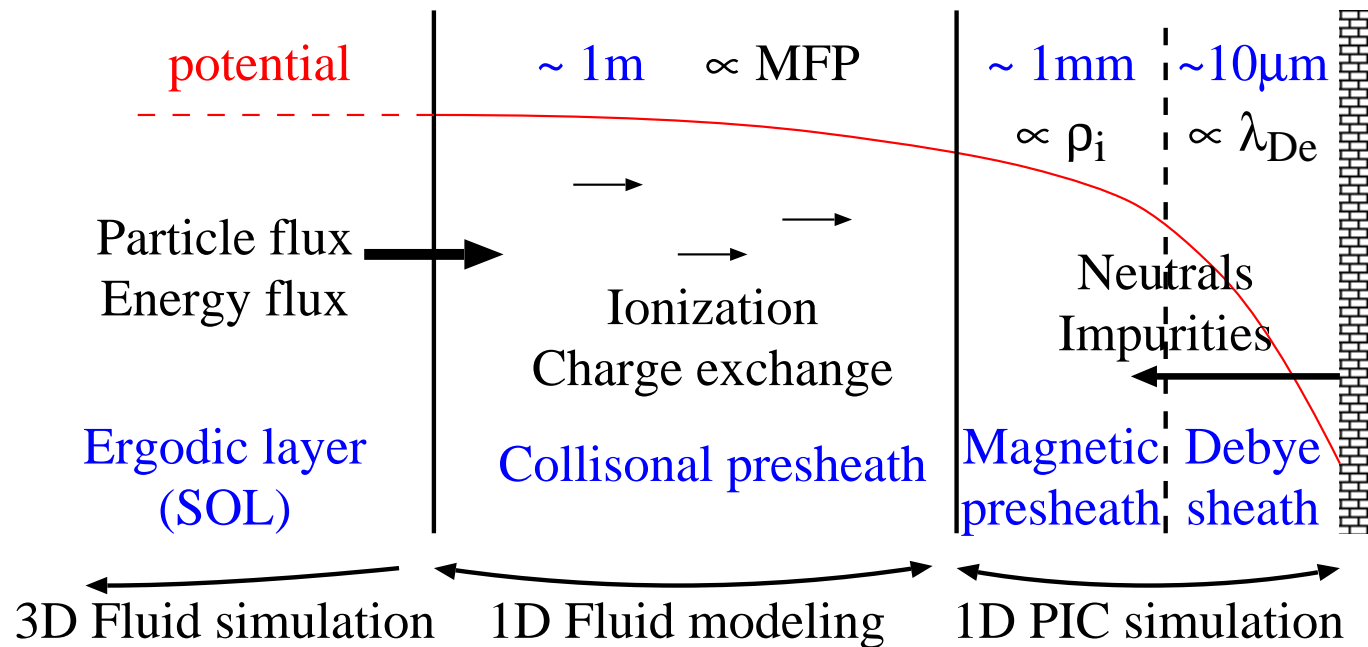
‡ wall configuration and grid generation

⇒ Modeling is necessary to apply the code to a new device.

Plasma modeling of the divertor leg*

§ Modeling and simulation of the divertor plasma

- † Parallel dynamics is dominant on the divertor plasma.
- † Braginskii equations along a flux tube is good approximation.
- † Interaction between plasma and neutral particles determines plasma profile.



*G. Kawamura et al., J. Plasma Fus. Res., 5 (2010) S1020

1D fluid equations of divertor plasma

§ Equilibrium equations solved numerically

$$\begin{aligned} \frac{d}{ds} [nv] &= S_n, \\ \frac{d}{ds} [m_i n v^2 + n(T_e + T_i)] &= S_p, \\ en \frac{d\phi}{ds} &= \frac{dnT_e}{ds} + 0.71n \frac{dT_e}{ds} - \frac{j}{\sigma_{\parallel}}, \\ \frac{d}{ds} \left[\frac{m_i n v^3}{2} + \frac{5}{2} n v T_i - \kappa_{\parallel i} \frac{dT_i}{ds} \right] &= -en v \frac{d\phi}{ds} + \frac{3m_e n}{m_i \tau_e} (T_e - T_i) + S_{Ei}, \\ \frac{d}{ds} \left[\frac{5}{2} n v T_e + q_{\text{lim}} \right] &= en v \frac{d\phi}{ds} - \frac{3m_e n}{m_i \tau_e} (T_e - T_i) - L r_{\text{imp}} n^2 + S_{Ee}, \\ \frac{1}{q_{\text{lim}}} &= \frac{1}{-\kappa_{\parallel e} \frac{dT_e}{ds}} + \frac{1}{\alpha n v_t T_e}. \quad \underline{\text{electron heat flux limit } (\alpha = 0.15)} \end{aligned}$$

s : spatial coordinate along B , n : plasma density ($n_e = n_i = n$), v : parallel flow velocity, S_n : particle source, T_e and T_i : electron and ion temperatures, S_p : momentum source, $\kappa_{\parallel i}$: ion heat conduction coefficient, S_{Ei} : ion energy source, $\kappa_{\parallel e}$: electron parallel heat conduction coefficient, τ_e : e-e collision time, $L = L(T_e)$: radiation cooling efficient, S_{Ee} : electron energy source.

Neutral model

§ Recycling and cascade processes of hydrogen

Wall surface

↓ release

H₂ molecules

↓ dissociation

H atoms

↕ IZ, CX, recombination

H⁺ ions

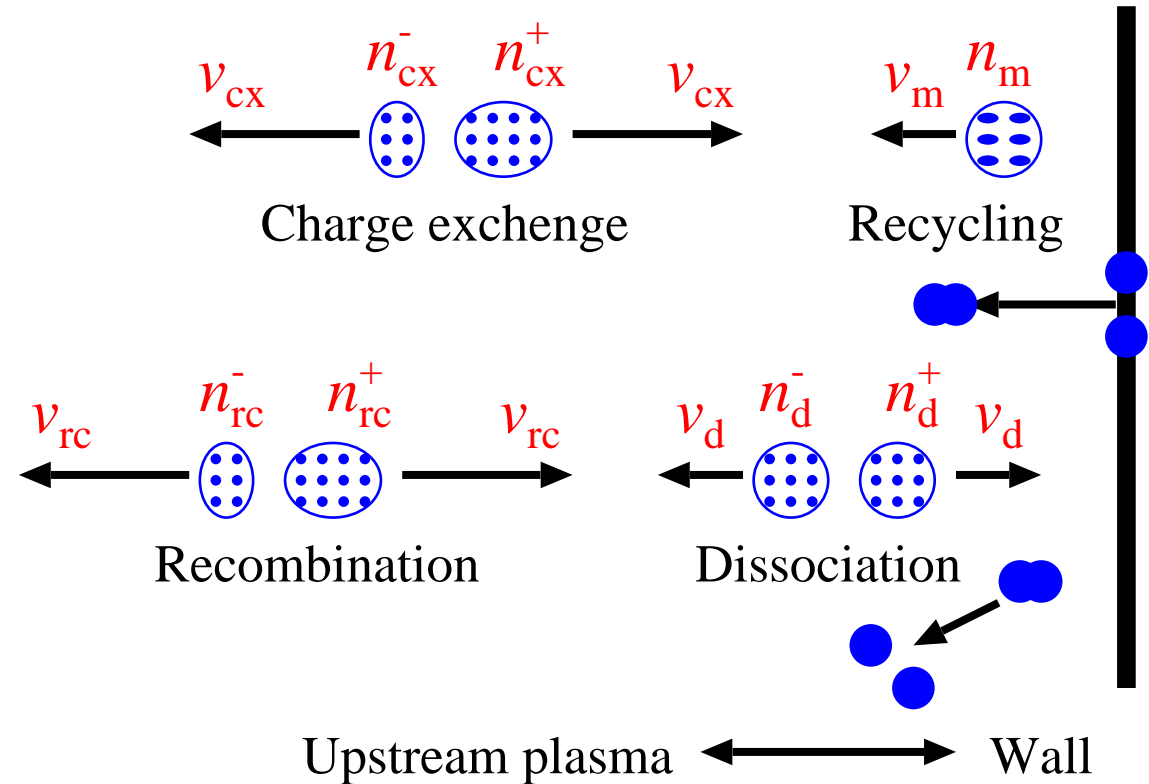
↓ surface recombination

Wall surface

n⁺ : downstream particle.

n⁻ : upstream particle.

§ Equilibrium equations



$$-v_m \frac{dn_m}{ds} = -(\langle \sigma_{d1} v \rangle + \langle \sigma_{d2} v \rangle) n_m n,$$

$$\pm v_d \frac{dn_d^\pm}{ds} = \dots, \quad \pm v_{cx} \frac{dn_{cx}^\pm}{ds} = \dots, \quad \pm v_{rc} \frac{dn_{rc}^\pm}{ds} = \dots$$

Plasma profile — an example

§ Plasma and neutral profiles

† Used parameters:

$$l_p = 3 \text{ [m]}, \quad \varphi = 80^\circ,$$

$$T_m = 600 \text{ K},$$

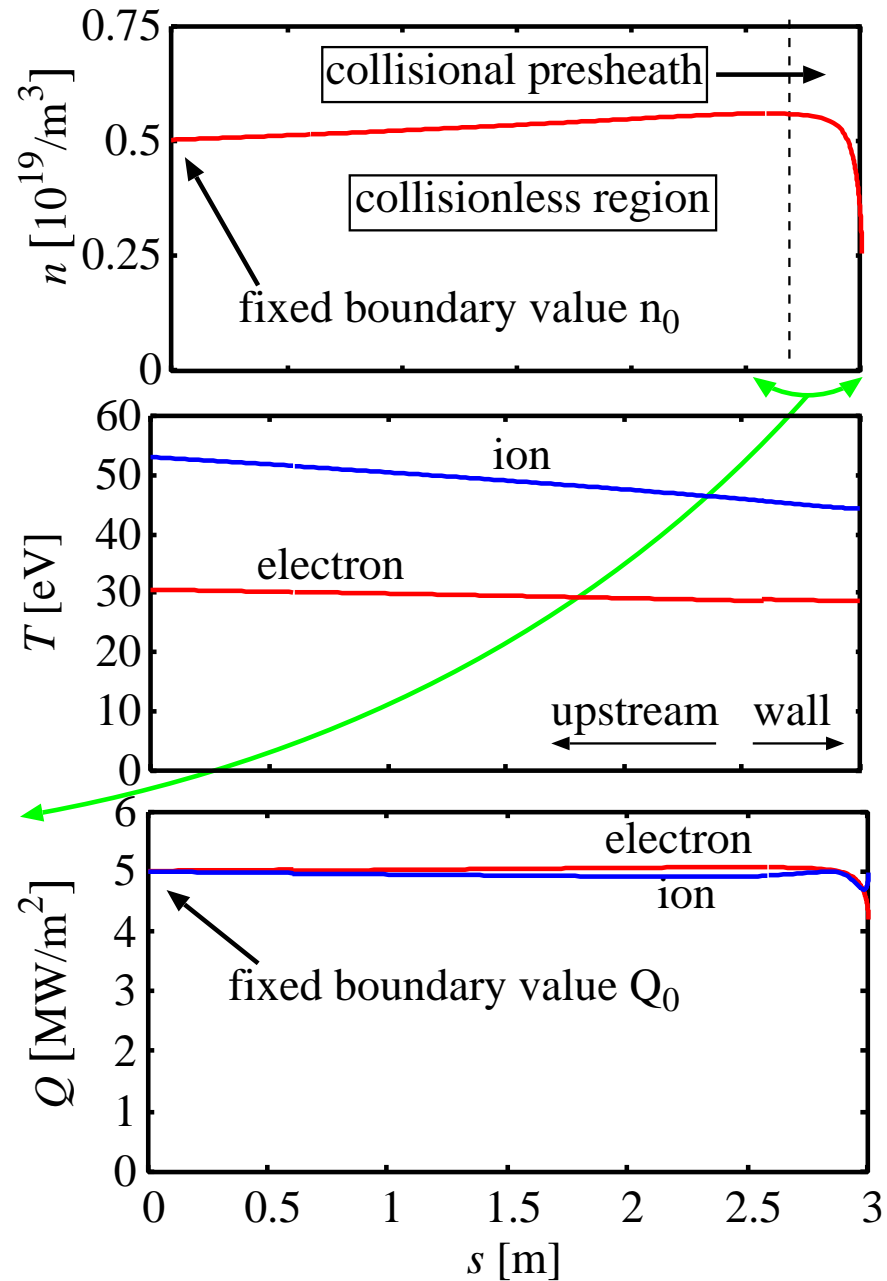
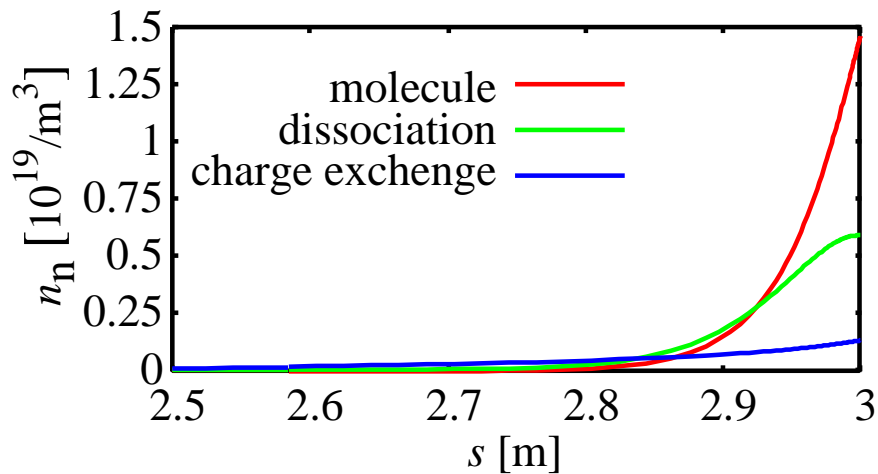
$$r_{pl} = 0.5, \quad r_{imp} = 0.03,$$

$$n_0 = 0.5 \times 10^{19} \text{ [m}^{-3}\text{]},$$

$$Q_0 = 10 \text{ [MW/m}^2\text{]}.$$

† Calculation time:

0.2~0.5 seconds on Core2Quad machine (Q9300 2.5GHz).



Plasma profile in ERO simulation

§ Background plasma

- † The divertor leg plasma is given by a 1D profile of a two-fluid model including interactions with neutral particles.
- † The perpendicular profiles to the center line of the divertor leg is given by a Gaussian shape,

$$T(l) \propto \exp(-l^2/\lambda^2),$$

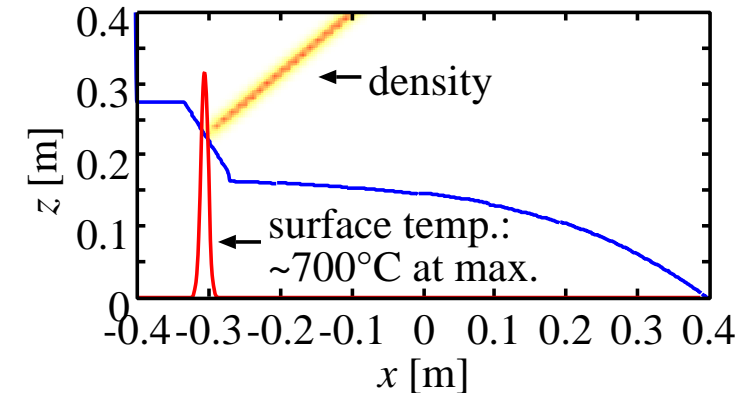
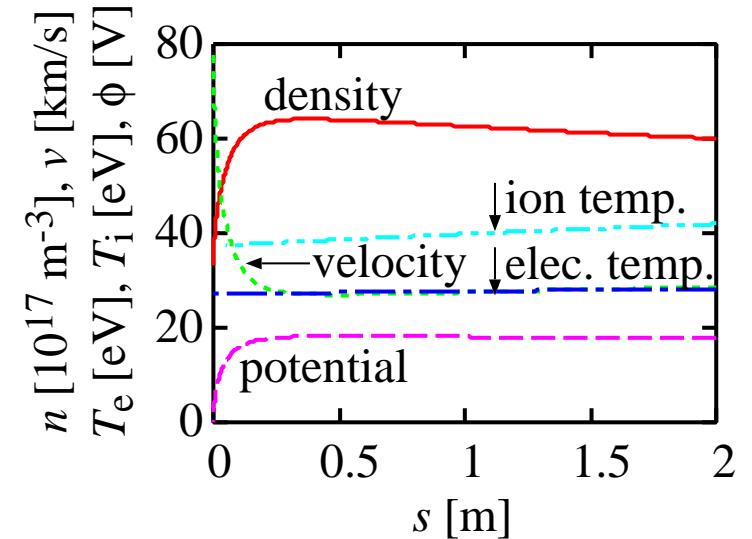
where characteristic length $\lambda = 1\text{cm}$.

- † Surface temperature is calculated from the power load on the surface,

$$Q_{\text{wall}} \propto nvT \propto n(T_e + T_i)^{3/2}.$$

§ Surface geometry

- † Surface is defined by a function $z(x)$.
- † Only one surface is available in the current version.



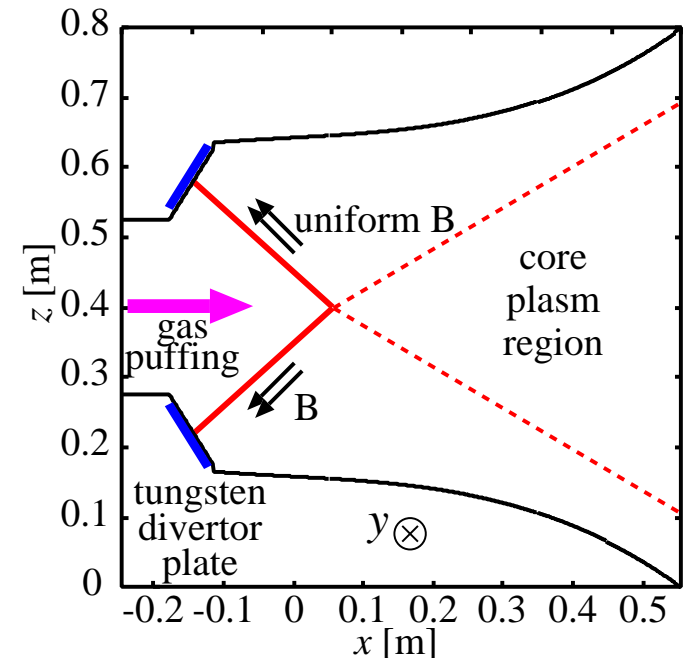
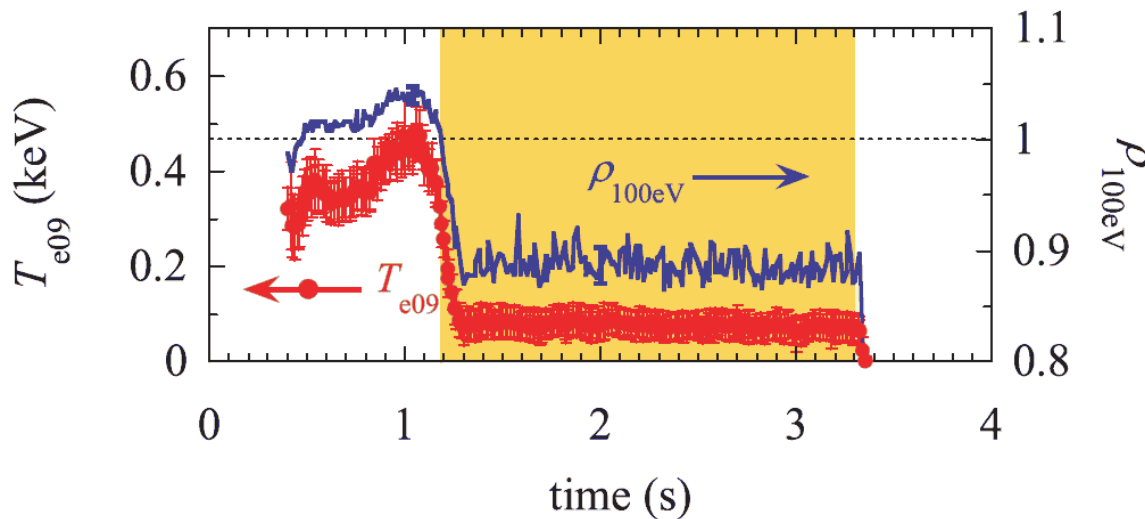
3. Gas puffing simulation

§ Background

- † Sustained detachment has been achieved with the aid of strong H gas puffing. The core plasma, however, becomes low temperature due to the excess source.
- † Neon and argon gas puffing is planned to expect larger radiation cooling and a preliminary test has been carried out successfully.

§ Objectives

- † Heavy ion causes large erosion of the divertor tiles even on tungsten.
- † Understanding of transport of the ions and estimation of the erosion are necessary task for advanced LHD discharges in future.

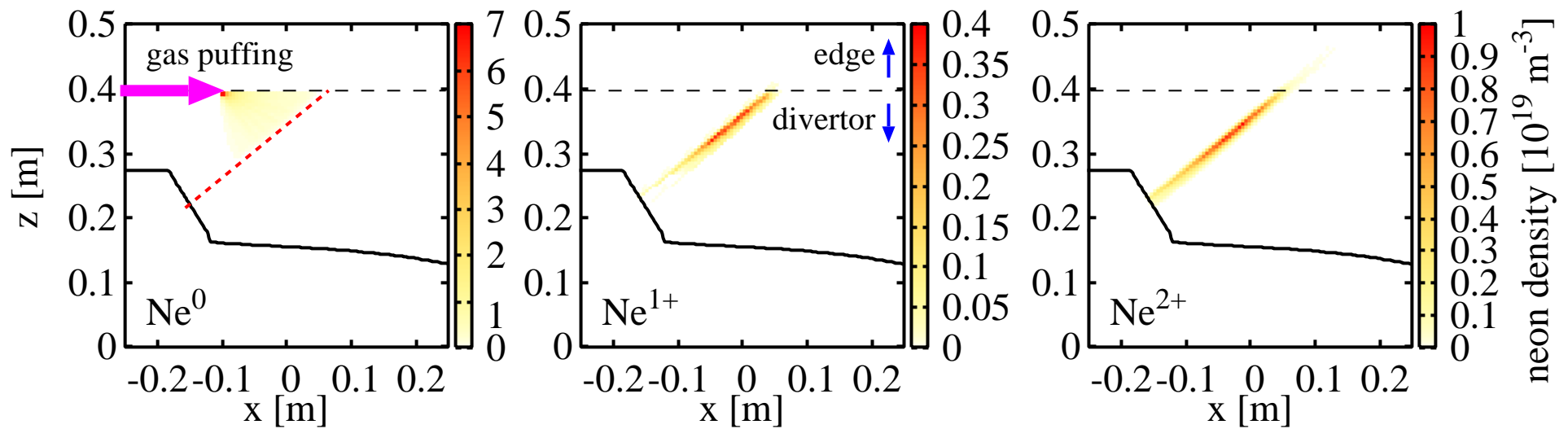


Detachment by strong hydrogen gas puffing

Neon transport

§ Spatial distributions of neon atom and ions

- † Flow rate of the neon gas: $1\text{Pam}^3/\text{s} = 2.7 \times 10^{20}$ atoms/s in 300 K.
- † The neon atoms are ionized immediately and flow toward the divertor tile.
- † The friction force is dominant.
- † Significant fluxes of Ne^{2+} and Ne^{3+} are observed on the surface.



Erosion and redeposition of tungsten

§ Erosion distribution of W tile along x -axis

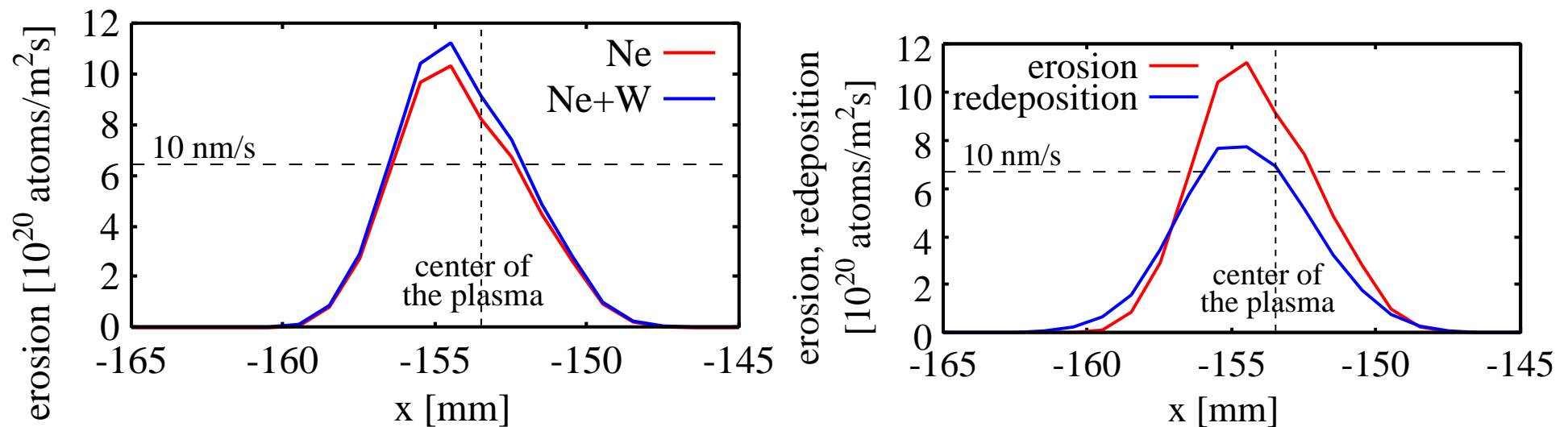
† Erosion by Ne bombardment $\sim 15\text{nm/s}$ for $1\text{ Pam}^3/\text{s}$.

† Erosion by W bombardment, i.e. self-sputtering, is not significant in this case.

§ Redeposition distribution of W tile along x -axis

† The effective erosion rate is around 1/3 of the pure erosion rate.

† Deposition region is observed outside the erosion region.



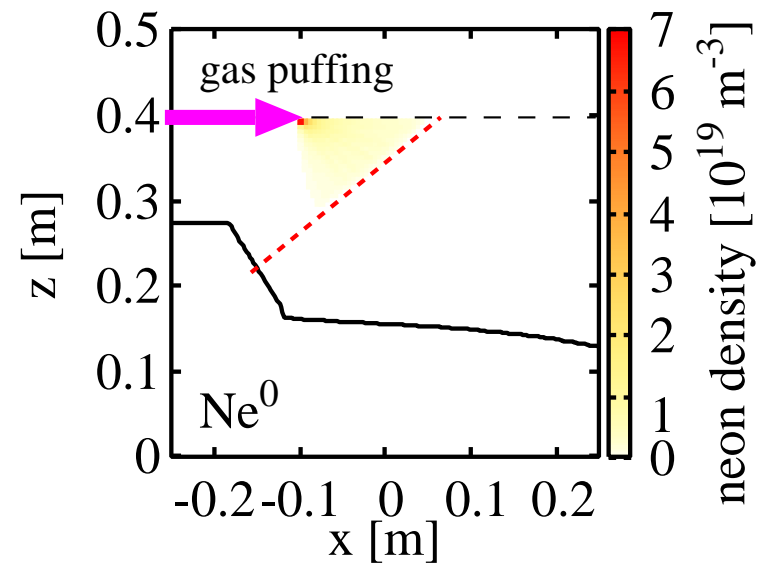
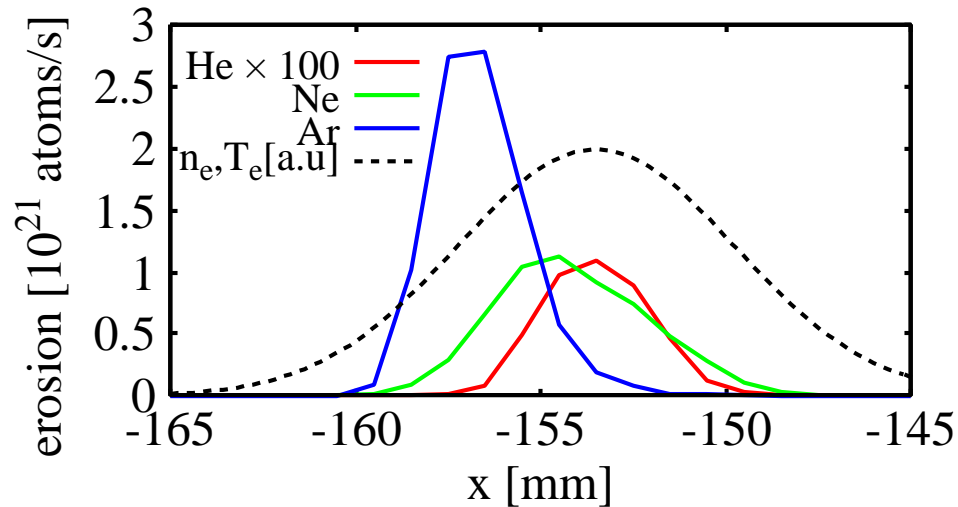
We note that the distribution can change for different cross-field diffusion coefficient.

No diffusion in this simulation.

Influence of different gas species

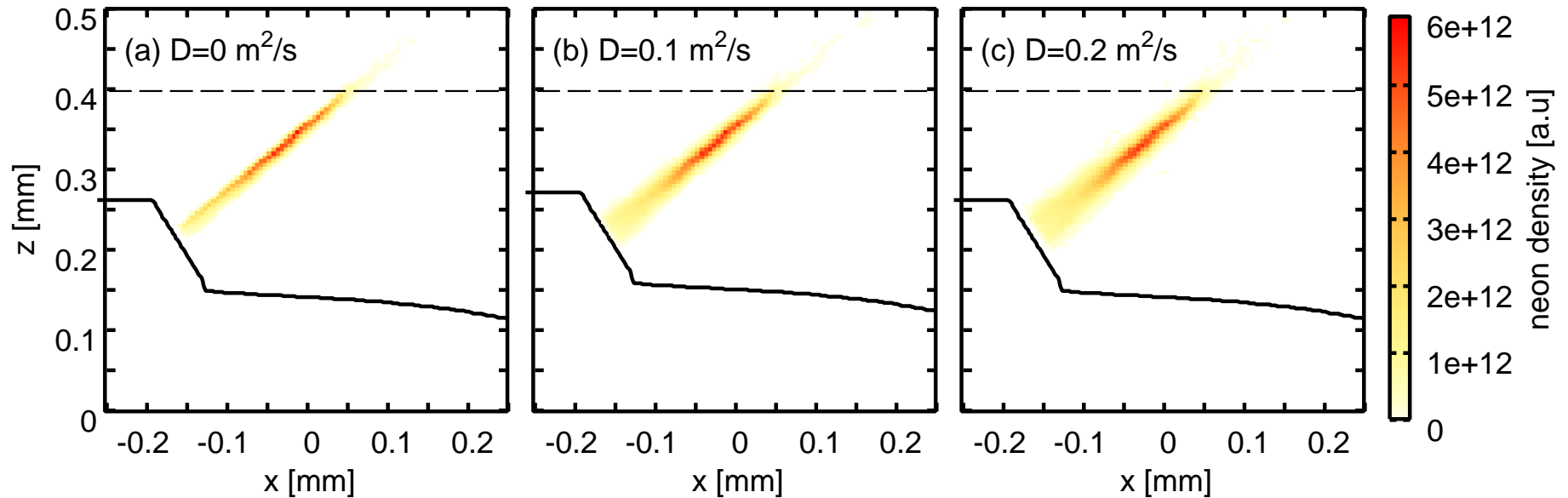
§ Helium, neon and argon puffing simulation

- † Erosion due to helium is negligibly small for the plasma of $T_e \sim 30\text{eV}$ because of the higher energy threshold.
- † Argon erodes tungsten two times more than neon.
- † The peak shift is caused by the higher ionization rate which makes ionizations in shallow position in the leg.
- † Ionization energy
He: 24.6eV, Ne: 21.6eV, Ar: 15.8eV.



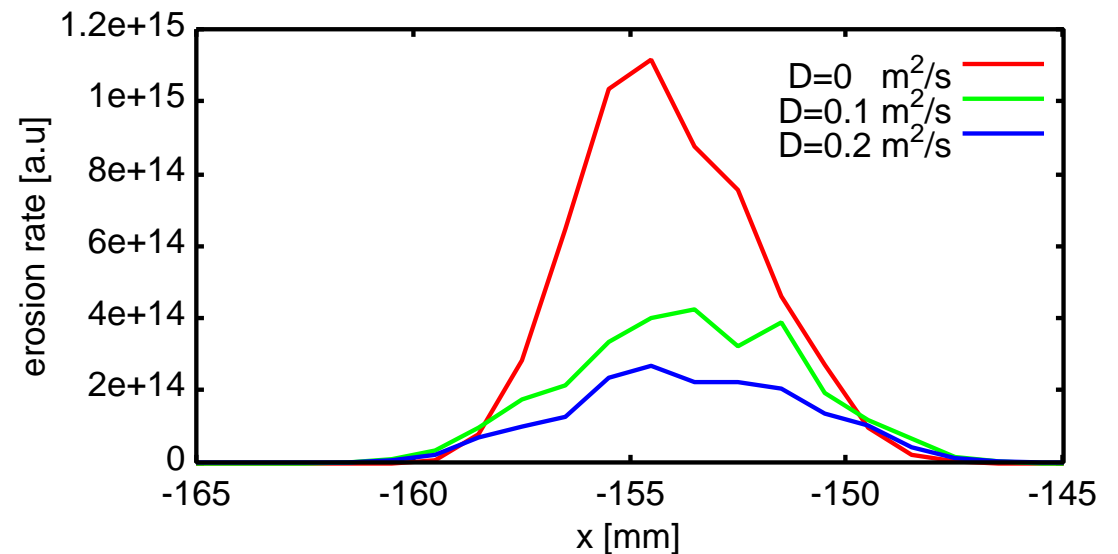
Perpendicular diffusion of impurity

§ Impurity distribution with constant diffusion coefficient



§ Erosion distribution

- † Large diffusion causes less erosion.
- † Diffusion model for the divertor leg is necessary.
- † Plasma modeling with diffusion is also important.



4. Summary

§ LHD divertor modeling for ERO

- † Plasma and wall configurations
- † 1D plasma modeling by two fluid equations

§ Gas puffing simulation

- † Upper limit of erosion and redeposition rate were estimated.
- † Effect of impurity diffusion was studied.

§ Future issues

- † Diffusion coefficient model of impurity in the divertor leg.
- † Advanced plasma modeling with EMC3.
 - ⇒ extension of the simulation grids to the legs
- † Integration of ERO and EMC3

